# Modeling Infrared Imaging in Biomaterials

**Justin Appel** **Andras Balogh** **Katherine Renee Fister**

**Magdalena Luca** **Zhi Ping Yang**

**Ellis Cumberbatch**
Claremont Graduate School
Problem Presenter

# 1 Introduction

The use of lasers in the medical fields is becoming more and more common. One example is the removal of port wine stain birthmarks. These birthmarks are abnormally large blood vessels that are very close to the surface of the skin. The most noticeable example is the large port wine stain birthmark on Gorbachev's head. Due to social and medical reasons it is sometimes beneficial to remove these birthmarks, but in the process it is also important not to scar the skin.

A diagnostic method to locate the depth and extent of the birthmarks uses pulsed photothermal radiometry (PPTR). In this method the birthmark is pulsed by a laser in which the frequency of the laser is set so that the blood vessels will absorb the heat and rise in temperature. Thus, once the birthmark has been pulsed by the laser, this area has an initial temperature distribution. This distribution is such that the blood vessels are at a higher temperature than the surrounding flesh. As the blood begins to cool the heat from the blood is conducted and radiated to the surface of the skin. The temperature changes in the flesh and blood as a result of the pulsed radiation are measured using an infrared detector which senses the radiation emitted. Due to the fact that radiation and thermal diffusion effects are coupled, determining thermal properties from a PPTR measurement, such as the initial temperature distribution, may be difficult and involve many mathematical questions.

A prominent working one-dimensional mathematical model has been developed by Milner *et al* [4] with promising results. This method is based on deriving an expression $S(t)$ in terms of the initial temperature distribution $U(z, t = 0)$ using the PPTR signal amplitude. The result is an inverse problem that can be solved using numerical methods to regain the initial temperature distribution.

The Milner *et al* results are based on the following model. The test material (skin, stain, flesh, etc.) occupies the zt-plane $z = 0 \longrightarrow \infty$ versus $t = 0 \longrightarrow \infty$, where $z$ is a spatial dimension with positive numbers going into the skin and $t$ is time. The heat loss is modeled by

$$\frac{\partial U}{\partial t} = D\frac{\partial^2 U}{\partial z^2}$$

where $U(z,t) = T(z,t) - T_a$ with $T(z,t)$ being the temperature in degrees Kelvin and $T_a$ the ambient temperature. The standard Robin boundary condition

$$\frac{\partial U}{\partial z}\Big|_{z=0} = hU\Big|_{z=0}$$

is used to model the radiative and thermal losses at the air-skin interface, where $h$ is the heat loss coefficient. These equations for heat transfer can be solved using Green's functions to get a closed form solution [2]

$$U(z,t) = \frac{1}{\sqrt{4\pi Dt}}\int_{z'=0}^{\infty} U(z',0)\left\{e^{\frac{-(z-z')^2}{4Dt}} + e^{\frac{-(z+z')^2}{4Dt}}(1 - h\sqrt{4\pi Dt}e^{u^2}\mathrm{erfc}(u))\right\}dz'$$

where $\mathrm{erfc}(u)$ is the complementary error function and $u = \frac{z+z'}{2\sqrt{Dt}} + h\sqrt{Dt}$. From this equation for the temperature distribution as a function of time and space it is possible to write the

measurement at $z = 0$ of the emitted radiation as a function of time which is weighted by the transmission loss in the flesh due to infrared absorption. Here the PPTR signal amplitude, the measured radiation, is given by

$$S(t) = C_d \mu \int_{z=0}^{\infty} U(z,t) e^{-\mu z} dz$$

where $\mu$ is the infrared absorption coefficient and $C_d$ is a proportionality constant. It is also important to note that the term $U(z,t)$ in $S(t)$ above is a linearization of the broad band radiation $\sigma T(z,t)^4$. The linearization is given by $\sigma(T(z,t)^4 - T_a^4) \approx \sigma 4 T_a^3 (T(z,t) - T_a) = \sigma 4 T_a^3 U(z,t)$ with the constants $\sigma 4 T_a^3$ absorbed into $C_d$. Now by using the expressions for $U(z,t)$ and $S(t)$ above and completing the integral over $z$ yields the following expression for $S(t)$ in terms of $U(z,0)$

$$S(t) = \frac{C_d \mu}{2} \int_{z'=0}^{z'=\infty} U(z',0) e^{\frac{-z'^2}{4Dt}} \left\{ \text{erfcx}(u_-) + \text{erfcx}(u_+) - \frac{2h}{h-\mu} (\text{erfcx}(u_+) - \text{erfcx}(u_1)) \right\} dz'$$

where $\text{erfcx}(u) = e^{u^2} \text{erfc}(u)$ is the exponential complementary error function and $u_{\pm,1}$ are given by $u_\pm = \mu\sqrt{Dt} \pm \frac{z'}{2\sqrt{Dt}}$ and $u_1 = h\sqrt{Dt} + \frac{z'}{2\sqrt{Dt}}$. The final equation for $S(t)$ can then be solved for $U(z,0)$ when the PPTR signal amplitude is known using different numerical techniques for inverse problems.

These results have been extended to three dimensions by Milner *et al* [5] under the assumption that longitudinal and lateral components of the temperature distribution can be separated.

The following paper deals with extensions and verifications of the models developed by Milner *et al* [4, 5]. It attempts to verify and develop several areas of the radiation model. Areas that are covered include narrow versus broad band radiation, addition of a radiation term in the original heat equation and different linearizations of the radiation. The paper also attempts to extend the previous results by developing different models for three dimensions. It ultimately attempts to develop a 3-D model of an individual blood vessel.

## 2 Notation

| Variable Name | | Variable Value |
|---|---|---|
| $\nu$ | = | $\frac{c_0}{n\lambda}$ |
| $[\nu]$ | = | $\sec^{-1}$ |
| $e_{b\lambda}\,\Delta\,\lambda$ | = | $e_{b\nu}\mid\Delta\nu\mid$ |
| $e_{b\nu}$ | = | $\alpha_1\left(e^{\frac{\alpha_2}{T}}-1\right)^{-1}$ |
| $e_{b\lambda}$ | = | $\alpha_1(e^{\frac{\alpha_2}{T}}-1)^{-1}$ |
| $\lambda$ | = | $b\mu$ |
| $[\lambda]$ | = | cm |
| $D$ | = | $\frac{k}{\rho c}$ |
| $D$ | = | $0.11\ \mathrm{mm}^2\cdot\sec^{-1}$ |
| $k$ | = | thermal conductivity |
| $[k]$ | = | $\frac{\mathrm{cal}}{\sec\cdot\mathrm{mm}\cdot{}^\circ\mathrm{K}}$ |
| $\rho$ | = | density of blood |
| $[\rho]$ | = | $\frac{g}{\mathrm{cm}^3}$ |
| $c$ | = | heat capacity |
| $[c]$ | = | $\frac{\mathrm{cal}}{\mathrm{g}\cdot{}^\circ\mathrm{K}}$ |
| $T$ | = | temperature in ° K |
| $T_a$ | = | ambient skin surface temperature in ° K |
| $T_0$ | = | body temperature in ° K |
| $U$ | = | $T-T_a$ |
| $V$ | = | $T-T_0$ |
| $\alpha_1$ | = | $\frac{c_1}{n\lambda^3 c_0}$ |
| $[\alpha_1]$ | = | $\frac{\mathrm{cal}}{\mathrm{cm}^2}$ |
| $\alpha_2$ | = | $\frac{c_2}{n\lambda}$ |
| $[\alpha_2]$ | = | °K |
| $M$ | = | $\frac{4}{3}\cdot\frac{\alpha_1\lvert\Delta\nu\rvert}{\rho c K_\lambda}$ |
| $[M]$ | = | $\frac{{}^\circ\mathrm{K}\cdot\mathrm{mm}^2}{\sec}$ |
| $M'$ | = | $M\alpha_2 T_0^{-2}e^{-\frac{\alpha_2}{T_0}}$ |
| $[M']$ | = | $\frac{\mathrm{mm}^2}{\sec}$ |
| $m$ | = | $\frac{\alpha_1\lvert\Delta\nu\rvert}{a\rho c}$ |
| $[m]$ | = | $\frac{{}^\circ\mathrm{K}}{\sec}$ |
| $2a$ | = | width of blood vessel |
| $a$ | = | 0.075 mm |
| $c_0$ | = | $2.998\times10^{10}\ \frac{\mathrm{cm}}{\sec}$ |
| $c_1$ | = | $3.740\times10^{-5}\frac{\mathrm{erg}\cdot\mathrm{cm}^2}{\sec}$ |
| $c_2$ | = | 1.4387 cm°K |
| $K_\lambda$ | = | $500\ \mathrm{cm}^{-1}$ |

# 3 Estimation of Various Effects

The goal is to examine possible deficiencies in the radiation model that the Milner *et al* [4] method may have. First, the idea is to analyze the time it takes for the absolute temperature $U_0$ in a blood vessel to decrease to $\frac{U_0}{2}$ through heat conduction and radiation separately. Secondly, the ratio of the radiation and conduction constants in the linearized heat equation is evaluated. Both of these estimates illustrate that radiation has a significantly lower effect on the problem than the heat conduction, even for early times in the problem. Thirdly, the significance of the Robin boundary condition is studied at high temperatures.

## 3.1 Basic Equations

The fundamental principle governing the temperature field within an absorbing and emitting medium is the same as that for a nonparticipating medium; that is, the expression of conversion of energy within the medium. When dealing with a radiation-participating medium, the model case in the port wine problem, the radiation flux within the medium must be added to the energy equation. The general equation for conversion of energy may be expressed as [9]:

$$\rho c \frac{\partial U}{\partial t} = \text{div } (k \text{ grad } U) + \beta U \frac{\partial p}{\partial t} + \mu \Phi - \text{div } \mathbf{q}_R$$

where $\beta$ is the coefficient of thermal expansion of the fluid, and $\beta = 0$ in the problem studied. Also, $\mu\Phi$ represents the irreversible work done on the element which is dissipated into heat as the result of fluid friction. Since fluid friction does not have a significant role in the port wine problem, the above equation reduces to the following one-dimensional form:

$$\rho c \frac{\partial T}{\partial t} = k \frac{\partial^2 T}{\partial z^2} - \frac{\partial}{\partial z}(q_R).$$

The monochromatic radiation flux is given by

$$\mathbf{q}_R = -\frac{4}{3K_\lambda} \text{grad } e_{b\lambda},$$

and

$$\mathbf{q}_R = \mathbf{q}_{R_\lambda} \triangle \lambda.$$

Thus, the above equations simplify into

$$\rho c \frac{\partial T}{\partial t} = k \frac{\partial^2 T}{\partial z^2} + \frac{4}{3} \frac{|\triangle \nu|}{K_\lambda} \frac{\partial^2}{\partial z^2} \left( \frac{\alpha_1}{e^{\frac{\alpha_2}{T}} - 1} \right),$$

or, combining constants,

$$\frac{\partial T}{\partial t} = D \frac{\partial^2 T}{\partial z^2} + M \frac{\partial^2}{\partial z^2} \left( \frac{1}{e^{\frac{\alpha_2}{T}} - 1} \right), \tag{1}$$

where the first term of the right-hand side represents conduction, and the second term represents radiation.

## 3.2 Heat Conduction versus Heat Radiation

For the heat equation,

$$\frac{\partial U}{\partial t} = D\frac{\partial^2 U}{\partial z^2},$$

where $D$ is the thermal diffusivity, consider the initial temperature distribution $U(z,0) = U_0$ in a blood vessel of width $2a$. From [2], the explicit solution to the above problem is

$$U(z,t) = \frac{1}{\sqrt{4\pi Dt}} \int_{-a}^{a} U_0 e^{\frac{-(z-s)^2}{4Dt}} ds.$$

The heat equation solution is analyzed at $z = 0$, giving

$$U(0,t) = \frac{U_0}{\pi} \int_{\frac{-a}{2\sqrt{Dt}}}^{\frac{a}{2\sqrt{Dt}}} e^{-y^2} dy$$

To determine the time it takes for the initial temperature $U_0$ to decrease by half, $\frac{U_0}{2}$ is substituted for $U(0,t)$ and the equation is solved for $t$. To solve for $t$, a Gaussian curve table shows that $\frac{a}{2\sqrt{Dt}} = 1.58$ [1]. Therefore, the time for the absolute temperature $U_0$ to decrease by a half is .005 seconds in the heat conduction case.

The effect radiation has on decreasing the absolute temperature $U_0$ by half is analyzed separately. For this, the radiation flux is viewed as

$$a\rho c\frac{\partial U}{\partial t} = \frac{\alpha_1}{e^{\frac{\alpha_2}{U-T_a}} - 1} \mid \Delta\nu \mid$$

Through approximation, the problem is

$$\frac{\partial U}{\partial t} = m\left(\frac{1}{e^{\frac{\alpha_2}{T}} - 1}\right)$$

For $\lambda = 10^{-3}$ cm, the specific constants are given below.

$$\alpha_1 = 5 \times 10^{-13} \ \frac{\text{cal}}{\text{cm}^2}$$

$$\alpha_2 = 1430 \ ^\circ\text{K}$$

$$\mid \Delta\nu \mid = 1.2 \times 10^{13} \ \text{sec}^{-1}$$

Furthermore, $m = 800 \ \frac{^\circ\text{K}}{\text{sec}}$

A chord approximation to the graph is used to analyze $\frac{\Delta U}{\Delta t} \approx m\left(\frac{1}{e^{\alpha_2/T} - 1}\right)$. Let $U_0 = 300$ °K since [4] uses a range of $T_0$ to be 273 to 313 °K. Then for simplicity let $\Delta U = 20$ °K. Hence,

$$\Delta t = \frac{20}{800}(e^{\frac{1430}{300}} - 1) = 2.9 \text{ seconds.}$$

Thus, the time it takes to decrease $U_0$ by half in the radiated problem above is 2.9 seconds. Comparatively, the heat conduction overrides the radiation even at early times by a factor of $10^3$ seconds.

## 3.3 Evaluation of $R_c$

The ratio of the radiation constant to the conduction constant in the linearized heat equation is $R_c$, Refer to section 4.3. The radiation coefficient in the linearized version is $M'$.

$$M' = Me^{-\frac{\alpha_2}{T_0}}\frac{\alpha_2}{T_0^2}$$

In particular, let $\lambda = 10^{-3}$ cm. Similar results are obtained for $\lambda$ in the ranges of $b = 3-5$ microns or $b = 7 - 11$ microns. Then $M = 1.6 \frac{^\circ\text{K mm}^2}{\text{sec}}$

$$M' = 2288e^{-\frac{1430}{T_0}}\frac{1}{T_0^2}\frac{\text{mm}^2}{\text{sec}}.$$

Now, $R_c = \frac{M'}{D}$. The concept is to determine at what temperature $T_0$ is $R_c >= 1$. Considering $R_c = 1$, we see that

$$\frac{-1430}{T_0} = -10 + 2\ln(T_0).$$

The graphs of $f(T_0) = \frac{-1430}{T_0}$ and $g(T_0) = 2\ln(T_0) - 10$ do not intersect. Therefore, the determination of $R_c$ must be visualized in the reasonable range of $T_0$. For $T_0 = 300$ °K, $M' = 2.2 \times 10^{-4} \frac{\text{mm}^2}{\text{sec}}$. Furthermore, $R_c = 2 \times 10^{-3} << 1$. Thus, the heat conduction dominates the radiation in the linearized version. So, the radiation term can be discarded in the heat transfer equation.

## 3.4 Importance of Robin Boundary Condition

In modeling the radiation from elevated temperatures it has been determined that initial measurement, generated by the highest temperatures do not fit the model developed by Milner *et al* [4, 5], and these measurements are not used. An interest has been expressed in developing a better model that would take into account these effects, especially for three dimensions. In developing the partial differential equations it is inherently easier if the Robin boundary condition

$$\frac{\partial U(z,t)}{\partial t} \mid_{z=0} = hU(z,t) \mid_{z=0}$$

can be disregarded. In short, it is important to find the effect of the heat loss coefficient $h$ ($h = 0.03\text{mm}^{-1}$ [4]). The effect of this boundary condition on the solution is determined in the following manner. First, the solution to the heat equation with initial conditions, $U(z,0) = c\delta(z - 0.4)$, is solved over $z = 0 \longrightarrow 2.5$ mm and $t = 0 \longrightarrow 5$ sec to obtain a

temperature profile in Fig. 1. The solution for this problem in an infinite domain is given by

$$U(z,t) = \frac{1}{\sqrt{4\pi Dt}} e^{\frac{-(z-0.4)^2}{4Dt}}$$

The next step is to solve the heat equation but this time incorporating the Robin boundary condition. The temperature profile for these equations is given in Fig. 2.

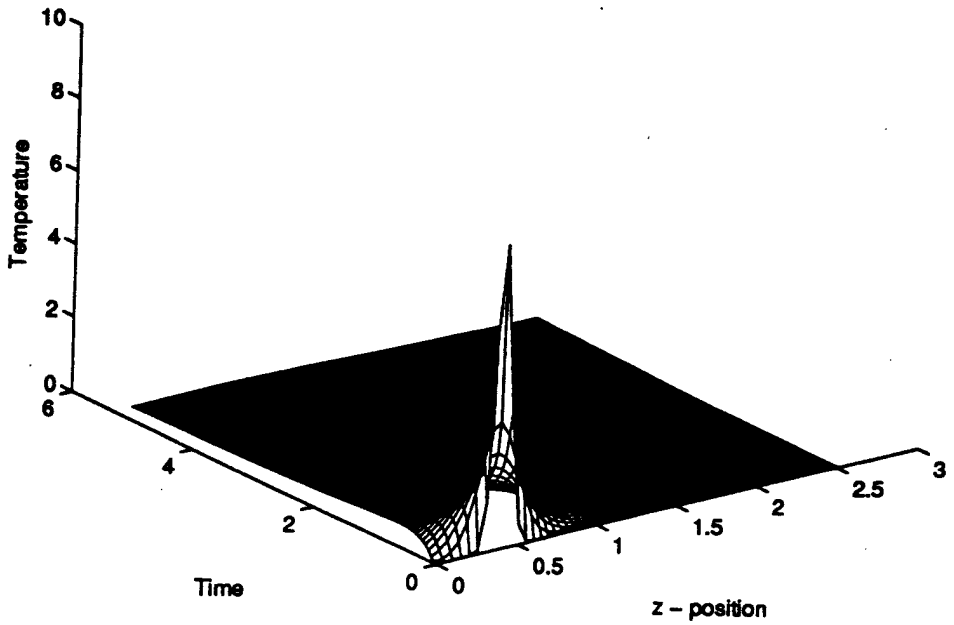


Figure 1: Solution of Heat Equation with no Robin boundary conditions

It is difficult to compare these graphs so the difference is plotted in Fig. 3. There seems to be a noticeable difference between the two solutions, but it is important to remember that our purpose here is to consider this difference only for high temperatures. Thus, for times when the temperature is high, the difference is very small. It appears that the largest difference appears at the air-skin interface boundary around time 1.5 seconds. Hence, it is reasonable to disregard the Robin boundary condition for high temperatures.

# 4 Analytical and Numerical Approaches

For the heat conduction and radiation problem, three concepts are utilized. First, a numerical scheme is analyzed for the fully nonlinear problem. Also, similarity solutions are discussed for the linear and the nonlinear problem. Then, the linearization of the nonlinear problem around $T_0$ is developed.

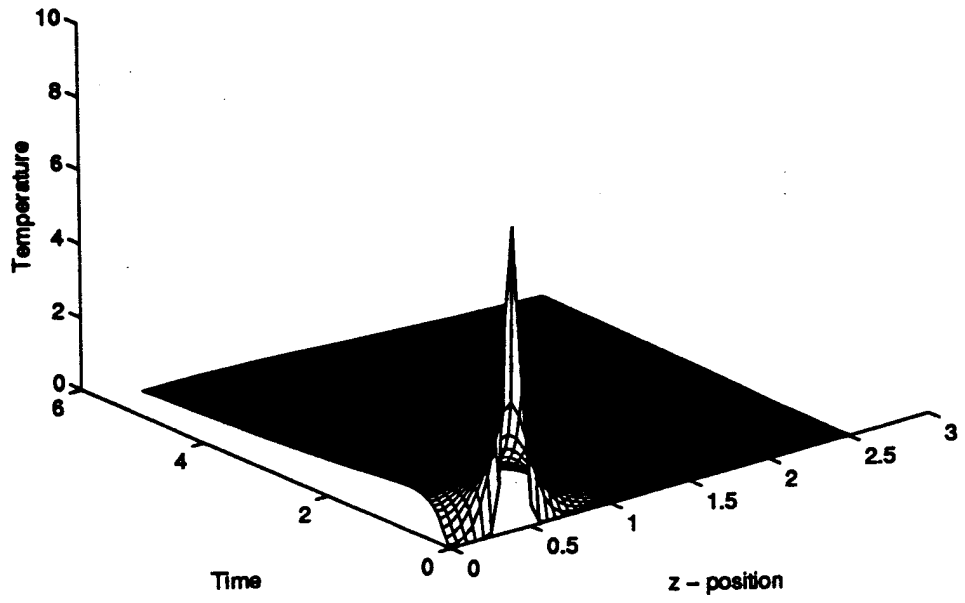


Figure 2: Solution of Heat Equation with Robin boundary condition

## 4.1 Numerical Solutions

In an attempt to determine the effect of the radiation term, it was conceivable to try to solve both the heat equation, Eq. 2 and the nonlinear heat equation, Eq. 1, using numerical techniques. In the short time frame it was not possible to write a code that would solve both equations. Thus, numerical techniques were limited to different "canned" packages. The first program invoked was the *IMSL* subroutine **MOLCH** which used the method of lines with cubic hermite polynomials. This program was able to solve the heat equation, but failed repeatably to solve the nonlinear heat equation, Eq. 1. The second program invoked was *XTC* by Bard Ermentrout. This program used a series of different numerical routines to try solve the problem. Once again it easily solved the heat equation but had some difficulty solving the nonlinear heat equation. After severely reducing the time step size, *XTC* was able to solve the nonlinear problem but the solutions of the two problems were nearly identical. The conclusion from the numerical results was that the difference between the solutions to the heat equation and the nonlinear heat equation with radiation was negligible and thus the radiation term could be disregarded.

## 4.2 Similarity Solutions

Eq. 1 can be analyzed using two separate equations: one linear, Eq. 2 and one nonlinear, Eq. 3.

$$\frac{\partial T}{\partial t} = D\frac{\partial^2 T}{\partial z^2}, \tag{2}$$

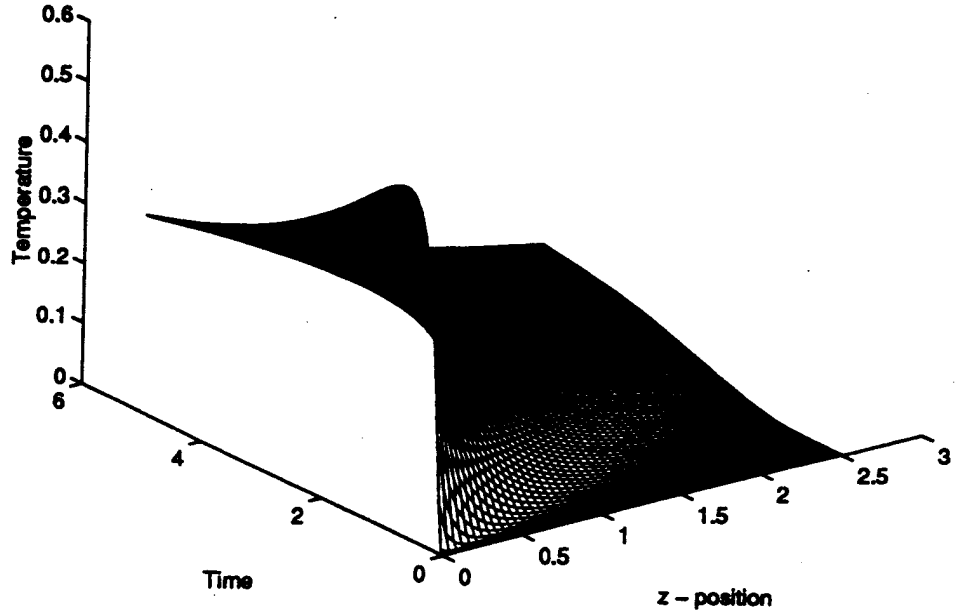


Figure 3: Temperature Difference profiles

$$\frac{\partial T}{\partial t} = M\frac{\partial^2}{\partial z^2}\left(\frac{1}{e^{\frac{\alpha^2}{t}} - 1}\right). \tag{3}$$

In order to solve these equations, similarity solutions are introduced. For Eq. 2, the following form is considered as a solution:

$$T = t^{\alpha} G\left(\frac{z^2}{tD}\right),$$

where $\alpha = -\frac{1}{2}$ is determined from the following dimensional analysis. Suppose the initial condition is $T(z,0) = c\delta(z)$.

$$[c] = \text{temperature} \star \text{length},$$

$$[\sqrt{Dt}] = \text{length}.$$

So

$$T = \frac{c}{\sqrt{Dt}} \star \text{non-dimensional function}.$$

Whence

$$\because \quad T = \frac{c}{\sqrt{D}} t^{-\frac{1}{2}} \star \text{non-dimensional function}.$$

Substituting into Eq. 2, we obtain the ordinary differential equation:

$$4uG'' + (2+u)G' + \frac{1}{2}G = 0$$

where $u = \frac{z^2}{Dt}$. The solution to this ODE is given by:

$$G = \hat{c}e^{-\frac{z^2}{4Dt}}.$$

Using $T(z,0) = c\delta(z)$, the following

$$T = \frac{c}{\sqrt{4\pi Dt}}e^{-\frac{z^2}{4Dt}}$$

is the solution of the linear differential equation, Eq. 2. The same approach is considered in order to solve equation, Eq. 3. For this equation,dimensional analysis indicates the solution representation is:

$$T = \frac{c^2}{Mt}\frac{1}{G(\frac{z}{\frac{Mt}{c}})}.$$

For the above mentioned nonlinear equation, the similarity solution does not simplify the initial equation to an ordinary differential equation, since the resulting equation is in terms of two variables. This result is due to the exponential function appearing in Eq. 3, and the form of $T$.

## 4.3 Linearization

Since the similarity solution for the nonlinear radiation problem fails, linearization of the partial differential equation is the next step. We note that the nonlinear term in Eq. 3 contains the absolute temperature, and typical temperature elevations are only fractions of the ambient body temperature. First, the denominator of the nonlinear term is approximated, where $T = U + T_a = V + T_0$ and $V << T_0$. Using a Taylor series approximation for $\frac{1}{V+T_0}$, the result is

$$\frac{1}{V+T_0} \approx \frac{1}{T_0} - \frac{1}{T_0^2}V$$

Then $e^{\frac{\alpha_2}{(V+T_0)}} - 1 \approx e^{\frac{\alpha_2}{T_0}}e^{-\frac{\alpha_2 V}{T_0^2}}$ where the 1 is discarded since it is negligible due to the size of $\alpha_2$ relative to $T$. Also,

$$\frac{1}{e^{\frac{\alpha_2}{(V+T_0)}} - 1} \approx e^{-\frac{\alpha_2}{T_0}}(1 + \frac{\alpha_2 V}{T_0}).$$

Substituting this approximation into Eq. 3, the partial differential equation becomes

$$\frac{\partial V}{\partial t} = M'\frac{\partial^2 V}{\partial z^2}$$

and the full equation Eq. 1, becomes

$$\frac{\partial V}{\partial t} = (D + M')\frac{\partial^2 V}{\partial z^2} \tag{4}$$

Let $D' = D + M'$. Then $D' = .109\ \frac{\text{mm}^2}{\text{sec}}$. Using previous results, the solution of Eq. 4 with $V(z,0) = c\delta(z)$ is

$$V = \frac{c}{\sqrt{4\pi D' t}} e^{\frac{-z^2}{4D't}}$$

In terms of the original $T$, the solution is given by

$$U = \frac{c}{\sqrt{4\pi D' t}} e^{\frac{-z^2}{4D't}} + T_0 - T_a$$

# 5 Broad Band versus Narrow Band Radiation

If $f(T) = 4n^2\sigma T_a^3(T - T_a)$ (broad band), $g(T) = \alpha_1 |\Delta\nu| \frac{\alpha_2}{T_a^2} e^{-\frac{\alpha_2}{T_a}}(T - T_a)$ (linearized narrow band) and $h(t) = (\frac{1}{e^{\frac{\alpha_2}{T}} - 1} - \frac{1}{e^{\frac{\alpha_2}{T_a}} - 1})\alpha_1 \mid \Delta\nu \mid$ (exact narrow band) are graphed in Fig. 4, then it is evident that the linearized narrow band radiation better approximates the exact narrow band radiation than does the linearized broad band radiation. If a comparison is made in ratio form of linear broad band to exact narrow band and linear narrow band to exact narrow band, then the former ratio is approximately 2.5 and the latter is approximately 1 for temperatures between 288 and 310 ° K as in Fig. 5. Hence, the linearized narrow band radiation is a better approximation to the exact narrow band radiation than what was previously used in Milner *et al* [4].

In Milner *et al* [4], a representation for $S(t)$, which is the measurement of the detected radiation, is given by

$$S(t) = C_d\mu \int_0^\infty U(z,t)e^{-\mu z}dz$$

Just as a note, the linearized broad band radiation means that the radiation has been integrated over all frequencies and then that quantity has been linearized. The narrow band radiation refers to the radiation term being linearized about the ambient temperature. For the partial differential equation

$$\frac{\partial U}{\partial t} = D\frac{\partial^2 U}{\partial z^2}$$

with initial conditions $U(z,0) = c\delta(z - d)$, the solution is given by

$$U = \frac{c}{\sqrt{4\pi D t}} e^{-\frac{(z-d)^2}{4Dt}}.$$

For broad band linearized radiation for any time,

$$S(t) = C_d\mu \int_0^\infty e^{-\mu z} n^2 \sigma 4 T_a^3 U dz$$

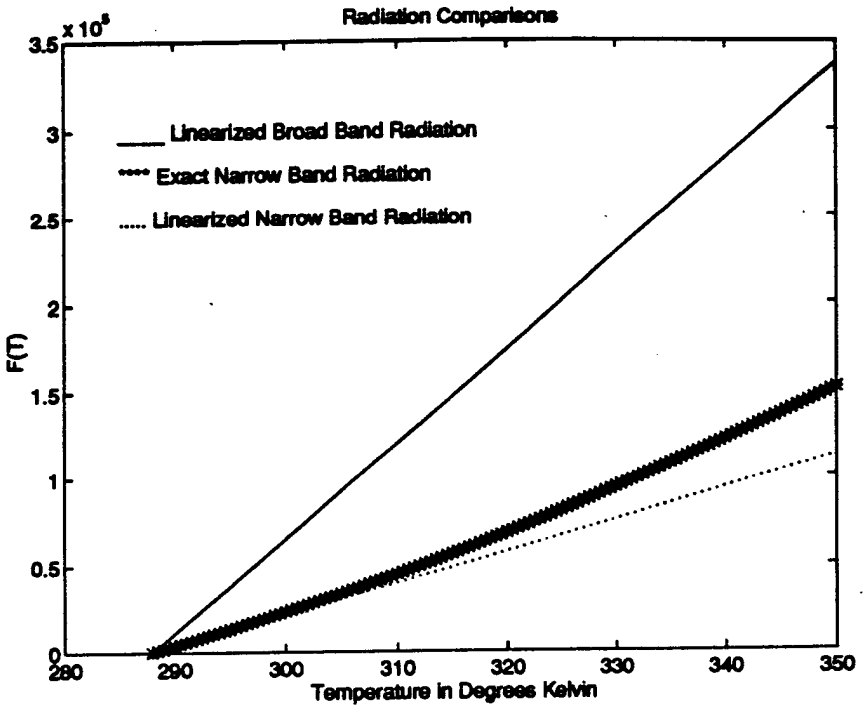


Figure 4: Comparison of Radiation Models

If a comparison is made to the narrow band radiation for times that are neither small nor large, then with $T > T_a$ and $\alpha_2 >> T$, linearization about $T_a$ is considered with $T = T_a + U$

$$e^{-\frac{\alpha_2}{T_a+U}} - e^{-\frac{\alpha_2}{T_a}} \approx e^{-\frac{\alpha_2}{T_a}} \frac{\alpha_2 U}{T_a^2}$$

Hence,

$$S(t) = \int_0^\infty \mu e^{-\mu z} e^{-\frac{\alpha_2}{T_a}} \frac{\alpha_2 U}{T_a^2} dz$$

Notice that the linearized broad band and the linearized narrow band radiation formulae differ by a multiplicative constant.

For the exact narrow band radiation,

$$S(t) = \mu \alpha_1 |\triangle \nu| \int_0^\infty e^{-\mu z} \left( \frac{1}{e^{\frac{\alpha_2}{T}} - 1} - \frac{1}{e^{\frac{\alpha_2}{T_a}} - 1} \right) dz.$$

# 6 Extensions to Three Dimensions

In [5] a mathematical model for the detection of infrared radiation was derived using the assumption that the initial three-dimensional temperature distribution is the product of two independent factors: a lateral and a longitudinal one. Let us consider a more general situation.

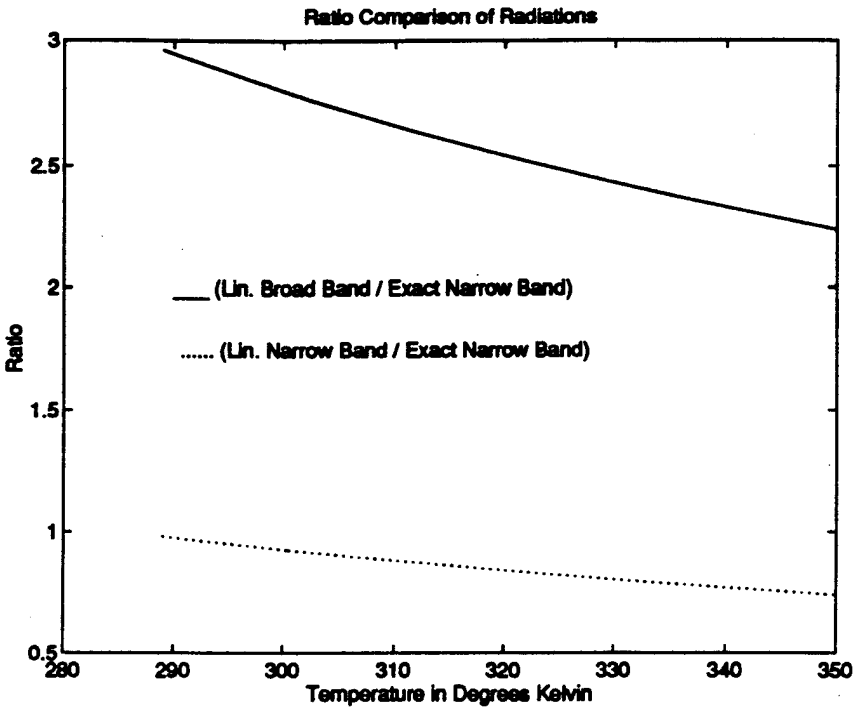


Figure 5: Ratio Comparison of Radiation Models

## 6.1 Net Radiation Exchange Between Surfaces

Physics books describe radiation as a surface property. Radiation flux and radiation intensity is measured per unit area. When we are given two surfaces, it is possible to calculate the net radiation exchange between the two surfaces. We have to consider the surfaces as the sum of differential area elements facing the direction of the output normal vector of the surface at the center of the differential area element. The result is that the net radiation arriving to one surface is a constant multiple of the net radiation emitted from the other surface. The constant multiplier is the so called view factor or configuration factor (see, e.g. [3] or [8]). There are the following difficulties with the application of this method to our problem:

- The surfaces need to be isothermal surfaces. In practice we do not know the location of isothermal surfaces after the irradiation. Assuming that the whole surface of the blood vessel is isothermal, we face the problem of determining the exact shape of the surface, and the corresponding view factor.
- The view factor is very complicated even for simple surfaces (like the configuration of two plates), and it depends on the shape of the surface.
- In order to obtain some kind of distribution of the radiation at the detector we should divide the surface of the detector into small parts, and calculate first the corresponding view factors, then the net radiation with respect to the small parts.

Refining the partition in the limiting case we end up with calculating the radiation per differential area element from a point to a point. We can calculate this directly, without the

viewing factor and without the limiting process.

## 6.2 Point-to-Point Radiation

(See [8], pp. 194-195 and [3], pp. 748-749) Let us assume that the radiation we are dealing with is diffusive, i.e., it is independent of the angle at which it leaves the surface. Consider a configuration (Fig. 6) where radiation arrives from a point $P_1 \equiv P_1(x, y, z)$ of the space to a point $P_2 \equiv P_2(\tilde{x}, \tilde{y}, 0)$ of the surface of the detector. (The detector is positioned in the $xy$-plane.) Consider a differential area element $dA$ around $P_1$ facing $P_2$, and differential area element $dS$ around $P_2$ in the plane of the detector's surface. Let $I$ be the intensity of the radiation leaving $dA$. Then the total radiation that leaves $dA$ and is intercepted by $dS$ is

$$Q_2 = I \; dA \; \cos\beta \; dw. \tag{5}$$

Here $\beta$ is the angle between the normal of $dS$ and the line segment of length $r$ joining $P_1$ and $P_2$, and $dw$ is the solid angle subtended by $dS$ when viewed from $P_1$. It denotes the area intercepted on the unit sphere with center $P_1$ by the oblique pyramid $P_1 dS$. Projecting $dS$ to obtain a surface parallel to $dA$, and using the fact that pyramids $P_1 dw$ and $P_1 \cos\beta dS$ are similar we obtain that

$$dw = \frac{dS \cos\beta}{r^2}$$

Substituting into Eq. 5 we obtain

$$Q_2 = \frac{I \; dA \; dS \; \cos\beta}{r^2}.$$

Finally, since the total diffuse energy leaving $dA$ within the entire hemispherical solid angle over $dA$ is $Q_1 = \pi \; I \; dA$,

$$Q_2 = \frac{Q_1 \; dS \; z}{\pi r^3}.$$

## 6.3 A Three-Dimensional PPTR Signal Model

Let us calculate the total radiation $S(x, y, t)$ absorbed at a point $(x, y)$ of the detector at a time $t$. A simplified version of Bougour's law says that the radiation decreases exponentially with distance, and we have to integrate through the half space to obtain

$$S(x, y, t) = C\mu \int_{-\infty}^{\infty} \int_{-\infty}^{\infty} \int_{0}^{\infty} Q(\xi, \eta, \zeta, t) \frac{\zeta e^{-\mu\sqrt{(x-\xi)^2+(y-\eta)^2+\zeta^2}}}{((x-\xi)^2 + (y-\eta)^2 + \zeta^2)^{\frac{3}{2}}} \; d\zeta \; d\eta \; d\xi. \tag{6}$$

Here $C$ and $\mu$ are absorption constants, $C$ depends on the detector and $\mu$ depends on the material. For the emitted radiation $Q(\xi, \eta, \zeta, t)$ we can substitute several formulas, according to the broad band, narrow band or linearized cases. Also, this expression can be studied as an inverse problem to obtain $U(x, y, z, t)$ at $t = 0$ from $S(x, y, t)$.

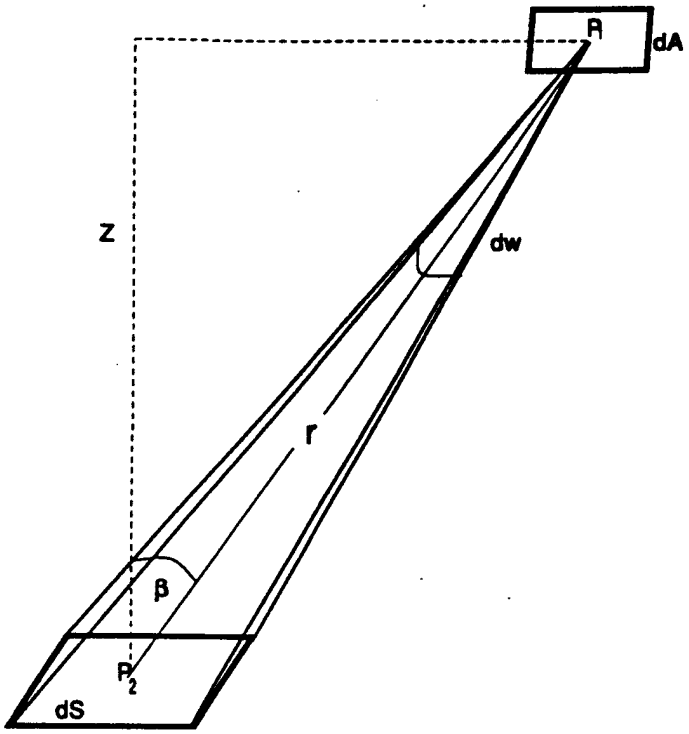


Figure 6: Radiation between two surfaces

## 6.4 The Complete Three-Dimensional Model

Blood vessels have sausage-like shapes, they are long, thin tubes. If we consider one of uniform cross-section and of finite length, we can build the general solution from that for a line delta function. That is, we can take an initial temperature distribution as

$$U(x,y,z,0) = \frac{q}{\rho c}\,\delta(y)\,\delta(z-z_o)$$

(The blood vessel is parallel to the $x-axis$).
We require the radiation from the temperature distribution to be derived from this initial input. A reasonable approximation for early times when the temperatures are highest is to neglect the boundary condition at $z=0$ (See Section 3.4).

The solution for the problem is

$$U(y,z,t) \equiv U(x,y,z,t) = \frac{q}{4\pi D\rho ct} e^{-\frac{[y^2+(z-z_o)^2]}{4Dt}}.$$

If we substitute this solution into Eq. 6 we obtain a formula for the PPTR signal

$$S(x,y,t) = \tilde{C}\int_{-\infty}^{\infty}\int_{-\infty}^{\infty}\int_{0}^{\infty} \frac{\zeta e^{-\frac{\eta^2+(\zeta-z_0)^2}{4Dt}} e^{-\mu\sqrt{(x-\xi)^2+(y-\eta)^2+\zeta^2}}}{((x-\xi)^2+(y-\eta)^2+\zeta^2)^{\frac{3}{2}}}\,d\zeta\,d\eta\,d\xi,$$

where $\tilde{C}$ is constant.

Notice that the integral is independent of $x$, hence we can write

$$S(y,t) = \tilde{C} \int_{-\infty}^{\infty} \int_{-\infty}^{\infty} \int_{0}^{\infty} \frac{\zeta e^{-\frac{\eta^2+(\zeta-\eta_0)^2}{4Dt}} e^{-\mu\sqrt{\xi^2+(y-\eta)^2+\zeta^2}}}{(\xi^2+(y-\eta)^2+\zeta^2)^{\frac{3}{2}}} \, d\zeta \, d\eta \, d\xi.$$

The radiation resulting from the initial temperature distribution can now be found by convolution.

# 7 Conclusions and Implications

The results illustrate that the nonlinear radiation term has a negligible effect on the heat transfer problem. The $R_c$ calculation and the time it takes for the initial temperature $T_0$ to decrease to $\frac{T_0}{2}$ supports this concept explicitly, as do the numerical results. Consequently, these considerations agree with the assumptions that Miller *et al* [4] made. It is important to note that the linearized narrow band radiation developed here is a better approximation to the exact radiation emitted and can easily be incorporated into the method of Milner *et al.*

# References


[1] Beyer, W., *CRC Standard Mathematical Tables, 25th Edition,* 1974, CRC Press, Inc., West Palm Beach, Ca.

[2] Carslaw, H.S. and J.C. Jaeger, *Conduction of Heat in Solids,* 1947, Oxford University Press, London, England.

[3] Incropera, F.P. and De Witt, D.P., *Fundamentals of Heat and Mass Transfer (3rd ed.),* 1990, Wiley, New York.

[4] Milner, T., D. Goodman, B. Tanenbaum, and J. Nelson, *Depth Profiling of Laser Heated Chromophores in Biological Tissues Using Pulsed Photothermal Radiometry,* 1995, preprint.

[5] Milner, T., D. Goodman, B. Tanenbaum, B. Anvari, and J. Nelson, *Noncontact Measurement of Thermal Diffusivity in Biomaterials Using Infrared Imaging Radiometry,* 1995, preprint.

[6] Özişik, M.N., *Radiative Transfer,* 1973, Wiley, New York.

[7] Özişik, M.N., *Boundary Value Problems of Heat Conduction,* 1968, International Textbook Co., Scranton, Ohio.

[8] Siegel, R. and Howell, J.R., *Thermal Radiation Heat Transfer,* 1972, Hemisphere Publishing Co., Washington.

[9] Sparrow, E.M. and R.D. Cess, *Radiation Heat Transfer,* 1978, Hemisphere Publishing Company, Washington.